

## Effect of North Pacific Storm Track on Winter Temperature in China

Hong-Yang Tseng,<sup>1</sup> Wei-Jun Zhu,<sup>2</sup> Chun-Juan Qi,<sup>3</sup> and Shyang-Yuh Wang<sup>4\*</sup>

<sup>1</sup>Department of Atmospheric Sciences, Chinese Culture University,  
55 Hwa Kong Road, Taipei City 111396, Taiwan

<sup>2</sup>School of Atmospheric Sciences, Nanjing University of Information Science & Technology,  
219 Ningliu Road, Nanjing, Jiangsu 210044, China

<sup>3</sup>Shanxi Meteorological Observatory, Xi'an, Shanxi 710014, China

<sup>4</sup>Department of Mass Communication, Chinese Culture University,  
55 Hwa Kong Road, Taipei City 111396, Taiwan

(Received August 27, 2021; accepted February 21, 2022)

**Keywords:** North Pacific storm track, weather forecasting, diagnosis, transient eddy dynamic forcing

Meteorological analysis and weather forecasting mainly rely on three essential elements, namely, data gathering, computing power, and theoretical solutions. The acquisition of data depends on various sensors and instruments. In this research, we utilized the singular value decomposition (SVD) analysis to analyze the data collected by the National Meteorological Information Center and the National Center for Environmental Prediction/National Center for Atmospheric Research (NCEP/NCAR) on the North Pacific storm track and winter temperature anomalies in China on the interannual scale. The results showed that the intensity change of the storm track was significantly and positively correlated with the temperature in most areas of China in winter. We also found that when the storm track weakens (strengthens), the winter temperature in China is generally lower (higher). Moreover, regression and composite analyses showed that the dynamic forcing along the storm track was important for the formation and maintenance of the atmospheric circulation. In addition, when the North Pacific storm track weakens (strengthens), the dynamic forcing of transient eddy is conducive to the maintenance of the positive (negative) phase of West Pacific (WP) teleconnection and leads to the deepening (filling) and southward (northward) movement of the East Asian trough and the strengthening (weakening) of the Siberia High and Aleutian Low. The forcing of transient eddy on the westerly flow tends to strengthen (weaken) the subtropical jet and weaken (strengthen) the westerly flow on the north side of the subtropical jet over the North Pacific. The anomalous centers of atmospheric circulation induced by the transient eddy are basically the same as that of the actual atmospheric circulation, which are conducive to the strengthening (weakening) of the winter monsoon, leading to a wide range of low-temperature weather in China.

---

\*Corresponding author: e-mail: [wxy6@ulive.pccu.edu.tw](mailto:wxy6@ulive.pccu.edu.tw)  
<https://doi.org/10.18494/SAM3602>

## 1. Introduction

The acquisition of data is a fundamental and the most upstream part of the overall key elements of data gathering for meteorological analysis and weather forecasting. Sensors are essential for collecting data, and these are widely used in ground observation instruments, radar, and satellites. The data collected by related equipment were reanalyzed, and the results were presented as grid point data. In this research, we utilized singular value decomposition (SVD) analysis to analyze the data collected by the National Meteorological Information Center and the National Center for Environmental Prediction/National Center for Atmospheric Research (NCEP/NCAR) on the North Pacific storm track and winter temperature anomalies in China on the interannual scale.

The synoptic-scale transient eddy is one of the important components of the atmospheric circulation system. It can affect weather by momentum, heat, and hydrological budgets over the midlatitude.<sup>(1)</sup> The synoptic-scale transient eddy has two zonal-extended regions with the most intensive variability in the midlatitude of the Northern Hemisphere, which are located in the North Pacific and North Atlantic, that is, the North Pacific and North Atlantic storm tracks. On an interannual time scale, the North Pacific storm track exhibits two principal modes, i.e., the monopole intensity change and the meridional shift of the storm track.<sup>(2)</sup>

In recent years, there have been many studies on the interaction between the synoptic-scale transient eddy and the low-frequency circulation over the midlatitude. The synoptic-scale transient eddies become developed owing to the perturbation kinetic energy transferred from the available potential energy in time-mean flow.<sup>(3)</sup> Moreover, synoptic-scale transient eddy activities affect the time-mean flow through the convergence of eddy momentum fluxes.<sup>(4,5)</sup> Some studies showed that Rossby wave breaking (RWB) plays important roles in eddy-mean-time flow dynamical interactions,<sup>(6)</sup> and anticyclonic events are beneficial to the northward migration of the western Pacific jet stream (WPJS).<sup>(7)</sup> Chen *et al.*<sup>(8)</sup> suggested that it is highly possible that the dynamical process through which the subtropical frontal zone (STFZ) affects WPJS is by the STFZ affecting the storm track and then causing the change in the WPJS via wave-mean flow positive feedback and RWB. Nakamura *et al.*<sup>(9)</sup> found that the enhanced poleward heat transport by the intensified storm track tended to be compensated for by the reduced transport by the weakened monsoonal flow over the northwestern Pacific. Zhang and Ren<sup>(10)</sup> showed that the transient eddy dynamic forcing anomalies are beneficial to establish and maintain the anomalous space type of the Aleutian Low on a low-frequency scale. Lau<sup>(11)</sup> pointed out that the storm track is linked to some monthly averaged teleconnection patterns. The dipolar western Pacific and western Atlantic patterns for the monthly mean flow are seen to be accompanied by marked changes in the intensity of the storm track over the western oceans, whereas the more wave-like Pacific/North American and eastern Atlantic teleconnection patterns are coincident with the meridional displacement of the storm track over the eastern oceans. Shi<sup>(12)</sup> showed that high-frequency transient eddy feedback forcing has an important impact on the evolution of East Asia-Pacific events through the geopotential height tendency equation.

The relationship between the storm track and ocean has also been extensively studied.<sup>(13–16)</sup> He *et al.*<sup>(17)</sup> found that the anomalous sea ice area over the southwest part of the Okhotsk Sea, together with the associated northern Pacific sea surface temperature anomaly (SSTA), can exert a crucial effect on the variability in the vigor and NW–SE extension of the Pacific storm track. SSTA may be one of the external forcing factors for the intensity change of the storm track. Liu *et al.*<sup>(18)</sup> reported that the strength and position variations of the wintertime Kuroshio Extension SST front have significant effects on the Pacific storm track. Sampe *et al.*<sup>(19)</sup> showed that an oceanic frontal zone acts to anchor a storm track, and its activity maintains the surface westerlies through its momentum transport. Wang *et al.*<sup>(20)</sup> and Fang and Yang<sup>(21)</sup> pointed out that it is via the enhanced subtropical oceanic front that the cooling mid-latitude SST anomalies can intensify the atmospheric transient eddy activities.

The winter temperature in China mainly depends on the East Asian winter monsoon (EAWM). The variations of the EAWM are mainly affected by the Siberian High and Aleutian Low systems. Some studies have pointed out that synoptic-scale transient eddy anomalies are closely related to the weather in China.<sup>(22,23)</sup> For example, Zhou *et al.*<sup>(24)</sup> found that there is a significant correlation between the cold wave frequency of China and the anomalous position of the Atlantic storm track in winter. Zhang and Qian<sup>(25)</sup> showed that the negative center of temperature transient anomalies in the lower troposphere can be traced as precursors to indicate the occurrence of regional prolonged low-temperature events in China in advance. Wang and coworkers<sup>(26,27)</sup> reported the relationship between the vertical and zonal structures of the North Pacific storm track in winter and the extreme low temperature in China. All the above studies suggest that the North Pacific storm track has some relationship with the weather in China, but few studies have mentioned the mechanism behind this. In this study, we will focus on the effect of the North Pacific storm track on winter temperature in China.

## 2. Data and Methods

In this study, we employed the global atmospheric circulation data, including monthly and daily geopotential heights, air temperatures, horizontal winds, and sea-level pressures from the National Center for Environmental Prediction/National Center for Atmospheric Research (NCEP/NCAR) reanalysis. These data have a horizontal resolution of  $2.5^\circ \times 2.5^\circ$  and a time span of 1961–2013. The daily average temperature dataset for 839 stations over China was provided by the National Meteorological Information Center.

SVD is an effective signal processing technique for analyzing nonlinear and nonstationary signals.<sup>(28)</sup> It is one of the methods for solving linear least-squares problems, which can be used to isolate the important coupled modes of variability between two fields.<sup>(29)</sup> This method has been used in many technical research studies,<sup>(30,31)</sup> and it is also widely used in the field of meteorological research. Gong *et al.*<sup>(32)</sup> used SVD analysis to reveal the linkage between the variations of the Siberian High and the East Asian surface air temperature. Shi *et al.*<sup>(33)</sup> studied the impact of the sea surface temperature anomaly in the Japan Sea and the sea area east of Japan on the winter rainfall and air temperature in Northeast China using SVD. Zhang *et al.*<sup>(34)</sup>

used this method to identify spatial air pollution index patterns related to meteorological conditions in China.

A 31-point digital filter was applied to obtain a synoptic-scale (2.5–6 days) transient eddy from the daily geopotential height field at 500 hPa.<sup>(35,36)</sup> Then, the monthly variance of the 500 hPa filtered geopotential height was calculated. Finally, the variance of the 500 hPa filtered geopotential height in winter for 52 years from 1961 to 2012 was obtained by calculating the winter average. In this paper, the variance of the 500 hPa filtered geopotential height represents the storm track. We mainly consider the effect of the North Pacific storm track on winter temperature in China on the interannual scale, so the harmonic analysis<sup>(34)</sup> was used to deal with the physical variables, and only their interannual component is retained.

To quantitatively describe the activities of the North Pacific storm track, following the definition of Li *et al.*,<sup>(37)</sup> we selected all grid points with the variance of the filtered geopotential height greater than or equal to a certain threshold. The average of the longitude and latitude of these grid points is defined as the longitude and latitude index of the storm track, and the average of all these grid points is defined as the intensity index of the storm track. In this paper, a certain threshold of the North Pacific storm track is 10 dagpm<sup>2</sup>. Additionally, the variance of the filtered geopotential height is weighted by area.

The teleconnection patterns used in this paper were from Wallace and Gutzler.<sup>(38)</sup> The West Pacific (WP) and Eurasian (EU) teleconnection pattern indices are defined as

$$WP = \frac{1}{2} Z^*(60^\circ\text{N}, 155^\circ\text{E}) - \frac{1}{2} Z^*(30^\circ\text{N}, 155^\circ\text{E}), \quad (1)$$

$$EU = \frac{1}{2} Z^*(55^\circ\text{N}, 75^\circ\text{E}) - \frac{1}{4} Z^*(55^\circ\text{N}, 20^\circ\text{E}) - \frac{1}{4} Z^*(40^\circ\text{N}, 145^\circ\text{E}). \quad (2)$$

Here,  $Z^*$  is the standardized 500 hPa geopotential height.

The East Asian winter monsoon index (EAWMI) was defined by Wang and Chen:<sup>(39)</sup>

$$IEAWM = (2 \times SLP_1^* - SLP_2^* - SLP_3^*) / 2, \quad (3)$$

where  $SLP_1^*$ ,  $SLP_2^*$ , and  $SLP_3^*$  indicate the normalized area-averaged SLP over Siberia (40°–60°N, 70°–120°E), the North Pacific (30°–50°N, 140°E–170°W), and the Maritime Continent (20°S–10°N, 110°–160°E), respectively.

The Kuroshio sea surface temperature index is based on the definition of Li and Sun,<sup>(40)</sup> which is defined as the average of SST over the region of 122°–150°E, 22°–36°N. Lau and Holopainen<sup>(41)</sup> advanced the forcing of the time-mean flow by transient eddies within the framework of a quasi-geostrophic equation. The geopotential height tendency of time-mean flow induced by the dynamic forcing of the synoptic-scale transient eddy can be expressed as<sup>(24,41–43)</sup>

$$\frac{\partial \bar{Z}}{\partial t} \propto -\frac{f}{g} \nabla^{-2} [\nabla_h \cdot (\overline{V' \zeta'})], \quad (4)$$

where  $V$  and  $\zeta$  represent the horizontal and vertical components of vorticity, respectively,  $f$  is the Coriolis parameter, the overbar is the mean flow component, and the prime is the transient component.

The zonal wind tendency of time-mean flow induced by the synoptic-scale transient eddy momentum flux can be written as<sup>(44)</sup>

$$\frac{\partial \bar{u}}{\partial t} \propto - \left( \frac{\partial(\overline{u'u'})}{\partial x} + \frac{\partial(\overline{u'v'})}{\partial y} + \frac{\partial(\overline{u'\omega'})}{\partial p} \right). \quad (5)$$

### 3. Relationship between North Pacific Storm Track and Winter Temperature in China

Figure 1 shows the climatological mean distribution and the first two empirical orthogonal function (EOF) modes of the variance of the 500 hPa filtered geopotential height during winter from 1961 to 2012. It can be seen that the climatological mean of the storm track distributes in an east–west band, with the main body over the North Pacific from 120°E to 120°W, and the maximum center is located west of the dateline near 40°N. The variance of the 500 hPa filtered geopotential height ranging from 30°–60°N to 120°E–120°W was taken to represent the North Pacific storm track. The first two EOF modes explain 28.1 and 18.5% of the total variance. These two modes can be separated from other modes on the basis of North *et al.*'s criteria.<sup>(45)</sup> Thus, we will focus on the spatial pattern and time coefficient of the first two modes. The spatial distribution of the first EOF mode [Fig. 1(a)] is mainly characterized by the same variability over the North Pacific. The correlation coefficient between the time series of EOF1 and the intensity index of the North Pacific storm track is 0.90, which is significant at the 99% confidence level, according to Student's *t*-test. Therefore, the first EOF mode mainly reflects the intensity change

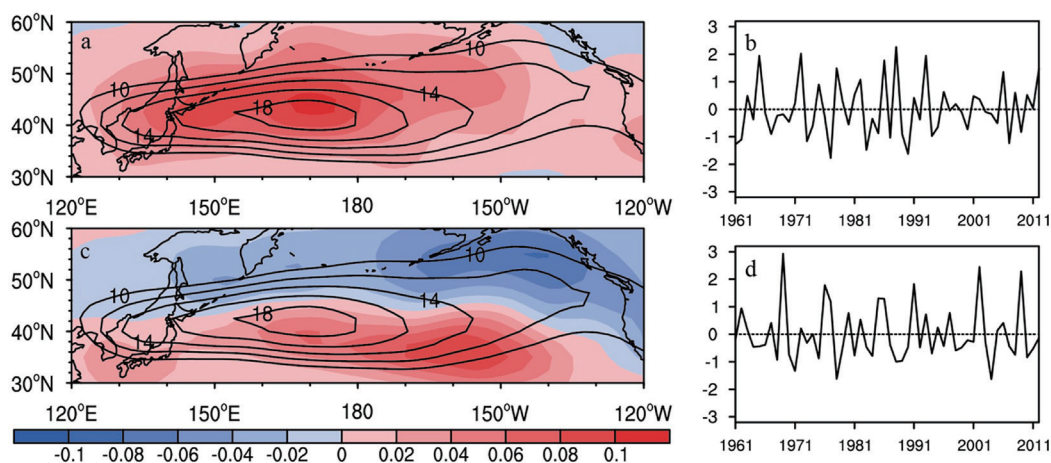


Fig. 1. (Color online) Spatial distributions of (a) EOF1 and (c) EOF2 of the variance of the 500 hPa filtered geopotential height for the 30°–60°N, 120°E–120°W region (shading) and its climatology (contour, unit: dagpm<sup>2</sup>) during winter from 1961–2012. Standardized temporal coefficients of (b) EOF1 and (d) EOF2.

of the storm track. The spatial distribution of the second mode [Fig. 1(c)] shows the reverse change of the north and south of the storm track, and the anomalous centers are all located east of the dateline. The correlation coefficient between the time series of EOF2 and the latitude index of the storm track is  $-0.90$ , which is significant at the 99% confidence level. Therefore, the second EOF mode mainly reflects the meridional movement of the storm track.

To examine the relationship between the North Pacific storm track and the winter temperature in China, we performed an SVD analysis on the variance of the 500 hPa filtered geopotential height anomaly (left field) in the North Pacific ( $30^{\circ}$ – $60^{\circ}$ N,  $120^{\circ}$ E– $120^{\circ}$ W) and the winter average temperature anomaly in China (right field) from 1961 to 2012. Figure 2 shows the typical spatial distributions of heterogeneous correlation. The first SVD mode (SVD1) accounts for 76.0% of the total square of covariance. The variance of the 500 hPa filtered geopotential height of SVD1 [Fig. 2(a)] shows that there is basically a negative correlation center over the climatological mean position of the storm track. The correlation coefficient between the time evolution of the left field of SVD1 and the intensity index of the storm track is  $-0.8$ , which is significant at the 99% confidence level. Therefore, the left field of SVD1 mainly reflects the intensity change of the North Pacific storm track. The corresponding distribution of the winter temperature field [Fig. 2(c)] has almost the same sign over China. It can be found that the left heterogeneous correlation [Fig. 2(a)] is greatly similar to the EOF1 pattern of the storm track [Fig. 1(a)] and the right heterogeneous correlation [Fig. 2(b)] is also greatly similar to the EOF1 pattern of the winter temperature in China (picture omitted), which indicates that their respective main modes are the most important coupling modes. The correlation coefficient of the time evolution of the left field with the right field is  $0.57$ , indicating that SVD1 mainly reflects the relationship between the intensity anomaly of the storm track and the winter temperature in

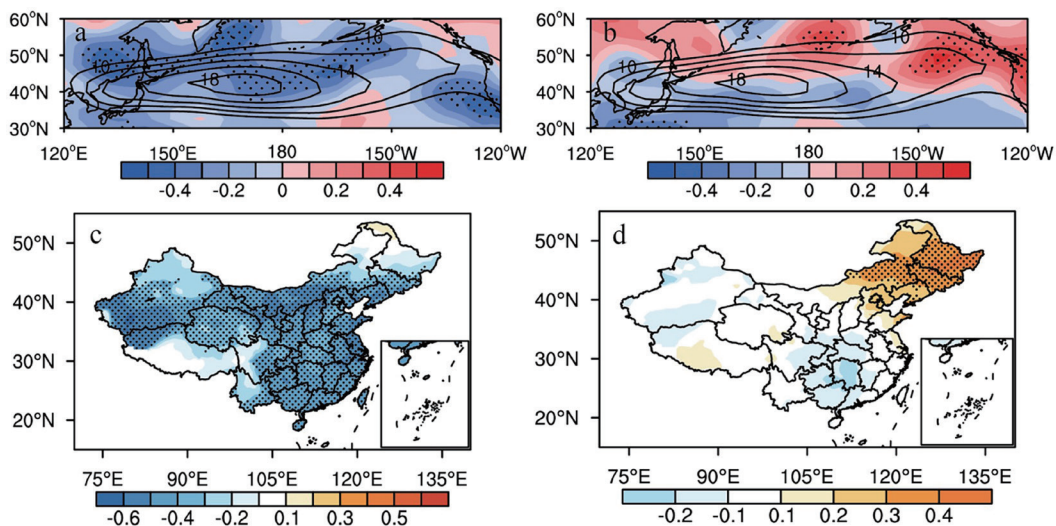


Fig. 2. (Color online) Heterogeneous correlation maps for the (a, c) first and (b, d) second SVD modes of the North Pacific storm track and the winter temperature in China from 1961 to 2012. The dotted areas represent correlation coefficients at/above the 95% confidence level. The solid lines (unit: dagpm<sup>2</sup>) represent the climatological mean of the North Pacific storm track in (a) and (b).

China. This means that when the North Pacific storm track weakens (strengthens) in winter, the temperature in China is lower (higher) than normal.

The second SVD mode (SVD2) explains 7.5% of the total square of covariance. For the left field of SVD2, there are three positive correlation centers in the north of the storm track and a negative center in the south of the storm track. The correlation between the time evolution of the left field of SVD2 and the latitude index of the storm track is 0.84, which is significant at the 99% confidence level. Therefore, the left field of SVD2 mainly reflects the meridional movement of the storm track. The corresponding distribution of the winter temperature field in Fig. 2(d) shows that the positive center is located in Northeast China, whereas the negative center is in Southwest China. The correlation coefficient between the time evolutions of the left and right fields of SVD2 is 0.59, which is significant at the 99% confidence level, so SVD2 mainly reflects the relationship between the meridional movement of the storm track and the winter temperature in China, that is, when the North Pacific storm track is northward (southward), the temperature anomaly in Northeast China is higher (lower), whereas that in Southwest China is lower (higher).

#### **4. Possible Mechanism of North Pacific Storm Track Affecting Winter Temperature in China**

The square of covariance of SVD2 is relatively small and the region passing the test of significance is small, so we focus on the mechanism of the first leading SVD mode. Although the North Pacific storm track is located downstream of China, it can still affect the climate of China through wave–flow interaction. To understand the possible mechanism of the North Pacific storm track affecting the winter temperature in China, the atmospheric circulation corresponding to the intensity anomaly of the storm track will be analyzed by regression and composite analyses.

##### **4.1 Variation of atmospheric circulation corresponding to intensity anomaly of North Pacific storm track**

Figure 3 shows the regression of 500 hPa geopotential height, 300 hPa zonal wind, sea-level pressure, and 850 hPa temperature field against the time evolution of the left field of SVD1. When the storm track weakens, significant negative geopotential height anomalies dominate the coast of Western Europe and the middle latitude from East Asia to the North Pacific, and the positive anomaly is zonally distributed in the high latitude area of Eurasia. The distribution of these anomalies bears good similarity to the positive phase of the EU pattern. The correlation coefficient between the left-field time evolution of SVD1 and the interannual component of the EU pattern is 0.51, which is significant at the 99% confidence level. Liu and Chen<sup>(46)</sup> found that the EU pattern in winter is closely related to the EAWM. When the EU pattern is in the positive phase, the EAWM is stronger and the temperature in East Asia is lower. Additionally, the meridionally oriented dipole pattern of the North Pacific is similar to the positive WP pattern. The correlation coefficient between the left-field time evolution of SVD1 and the interannual component of the WP pattern is 0.59, which is significant at the 99% confidence level. Li *et*

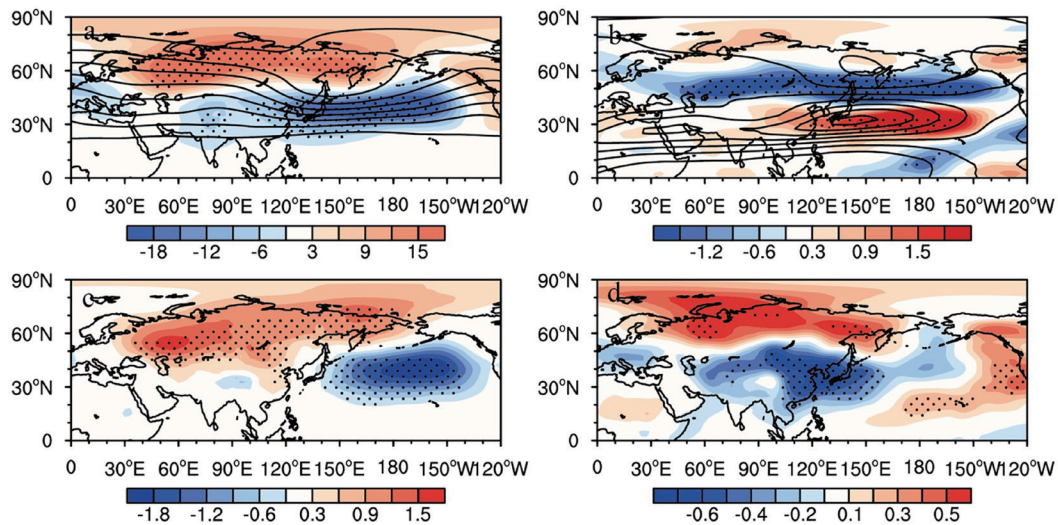


Fig. 3. (Color online) Regression of (a) 500 hPa geopotential height (unit: gpm), (b) 300 hPa zonal wind (unit:  $\text{m}\cdot\text{s}^{-1}$ ), (c) sea-level pressure (unit: hPa), and (d) 850 hPa temperature (unit:  $^{\circ}\text{C}$ ) against the time evolution of the left field of SVD1. The dotted areas indicate that the regression coefficient is statistically significant at/above the 95% confidence level by Student's  $t$ -test. The solid lines represent the climatological mean of 500 hPa geopotential height and 300 hPa zonal wind in (a) and (b).

*al.*<sup>(47)</sup> pointed out that the positive WP pattern shows negative anomalies in the middle-high latitude at the 500 hPa height field, and the circulation shows a zonal pattern. (Note that their definition of WP index is opposite to ours.) Accordingly, the EAWM weakens and the winter temperature in China is lower.

The zonal wind at 300 hPa [Fig. 3(b)] agrees with the geopotential height field [Fig. 3(a)]. It is clear that the subtropical westerly jet significantly strengthens, whereas the polar front jet weakens. The westerly wind anomalies together with the meridional circulation are conducive to the southward invasion of cold air.

The sea-level pressure field [Fig. 3(c)] is similar to the 500 hPa geopotential height field [Fig. 3(a)]. There is a positive anomaly in the middle-high latitude of Eurasia and a negative anomaly in the North Pacific, which means that the Siberia High strengthens and the Aleutian Low deepens, and it is beneficial to intensify the EAWM. The correlation between the left-field time evolution of SVD1 and the interannual component of EAWMI is 0.65, which is significant at the 99% confidence level. Correspondingly, a cold mass is formed in the south of Lake Baikal at the 850 hPa temperature field [Fig. 3(d)], and the weather in East Asia is affected by cold air.

Therefore, considering the above factors, when the North Pacific storm track weakens in winter, the main characteristics of the abnormal atmospheric circulation are the positive EU and WP patterns, meridional circulation in the middle-high latitude at 500 hPa, weakening polar front jet and strengthening subtropical jet at 300 hPa, and intensified Siberia High and Aleutian Low at sea-level pressure, which make the EAWM stronger. Moreover, a cold mass is formed in the south of Lake Baikal, which affects most parts of China, and results in low-temperature weather.



## 4.2 Possible mechanisms of North Pacific storm track affecting atmospheric circulation

Previous studies have shown that the synoptic-scale transient eddy is of great importance to the formation and maintenance of atmospheric circulation. In the following work, the possible mechanism of the intensity anomaly of the storm track affecting the time-mean flow will be discussed by analyzing the transient eddy-induced geopotential height and zonal wind tendencies according to Eqs. (4) and (5). First, the time evolution of the left field of SVD1 is standardized. The years when the absolute value of time coefficients is greater than one standard deviation are regarded as extreme abnormal years. The abnormal strong years of the storm track are nine years (1961, 1967, 1977, 1983, 1985, 1989, 1990, 2007, and 2009) and the abnormal weak years are eight years (1965, 1972, 1978, 1986, 1988, 1993, 2006, and 2012).

Figures 4(a) and 4(b) are the differences in the geopotential height and zonal wind tendencies induced by transient eddy dynamic forcing at 500 hPa between the storm track weak and strong years. As shown in the difference in geopotential height tendency [Fig. 4(a)], when the North Pacific storm track weakens, there is a dipole with the reverse signs in the North Pacific, which corresponds well to the regression of the 500 hPa geopotential height field [Fig. 3(a)]. This dipole structure is conducive to the maintenance of the positive WP pattern, which is one of the most important teleconnections modulating the EAWM. Tanaka *et al.*<sup>(48)</sup> pointed out that when the WP pattern is in the positive phase in winter, the enhanced northwesterly wind is enhanced by the positive phase of the WP pattern in winter. The significantly negative anomaly center is

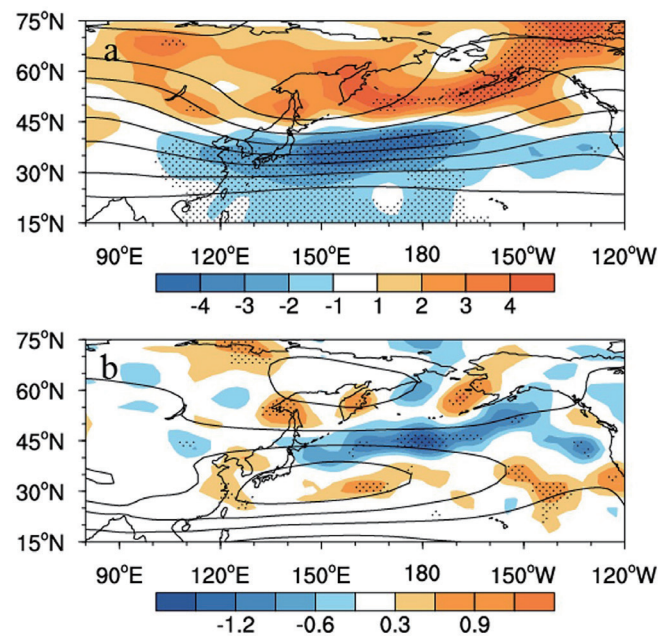


Fig. 4. (Color online) Differences in composited (a) geopotential height tendency (shading; unit:  $10^{-5} \text{ gpm}\cdot\text{s}^{-1}$ ) and (b) zonal wind tendency (shaded; unit:  $10^{-5} \text{ m}\cdot\text{s}^{-2}$ ) induced by transient eddy dynamic forcing at 500 hPa between the storm track weak and strong years. The dotted areas exceed the 95% confidence level according to Student's *t*-test. The solid lines represent the climatological mean of 500 hPa geopotential height and 300 hPa zonal wind in (a) and (b).

located in the south of the climatological mean of the East Asian trough, which indicates that the dynamic forcing of the transient eddy would deepen the East Asian trough and shift it southwardly. When the storm track weakens, there are a belt of negative zonal wind tendency anomaly near  $40^{\circ}\text{N}$  and positive anomalies on both north and south sides of  $40^{\circ}\text{N}$  [Fig. 4(b)], indicating that the subtropical jet strengthens and the westerly flow in the north of the subtropical jet weakens.

The winter temperature in China is mainly affected by the East Asian winter monsoon. Aleutian Low, as one of the important members of the winter monsoon circulation, has a clear effect on the EAWM. Yao *et al.*<sup>(3)</sup> showed that the transient eddy dynamic forcing anomalies are beneficial for establishing and maintaining the anomalous space type of the Aleutian Low on a low-frequency scale. Figure 5 shows the differences in geopotential height and zonal wind tendencies induced by transient eddy dynamic forcing at 850 hPa between the storm track weak and strong years. It can be seen from Fig. 5(a) that the anomalous centers of geopotential height tendency are basically consistent with the actual geopotential height anomalies. When the storm track weakens, the positive geopotential height tendency anomalies appear in the middle- and high-latitude areas of Eurasia, which indicates that the Siberian High strengthens, and the negative anomaly center is located in the south of the climatological mean of the Aleutian Low, which indicates the southward movement and deepening of the Aleutian Low. It can be found from Fig. 5(b) that the negative anomalies of the zonal wind tendency occur north of  $40^{\circ}\text{N}$  and the positive anomalies occur south of  $40^{\circ}\text{N}$ . The zonal wind tendency is adjusted with the

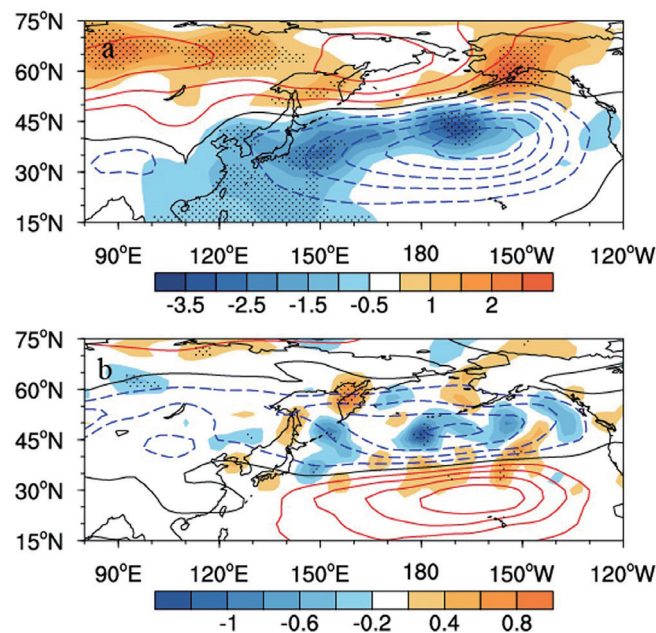


Fig. 5. (Color online) Differences in composited (a) geopotential height tendency (shading; unit:  $10^{-5} \text{ gpm}\cdot\text{s}^{-1}$ ) and (b) zonal wind tendency (shaded; unit:  $10^{-5} \text{ m}\cdot\text{s}^{-2}$ ) induced by transient eddy dynamic forcing at 850 hPa between the storm track weak and strong years. Dotted areas exceed the 95% confidence level according to Student's *t*-test. The lines represent the differences in composited (a) geopotential height and (b) zonal wind between the storm track weak and strong years.

geopotential height tendency. Thus, we can infer that when the storm track weakens, the dynamic forcing of transient eddy results in the intensification of the Siberian High and the deepening and southward movement of the Aleutian Low, which is conducive to the enhancement of the EAWM.

The above analyses show that the transient eddy along the storm track has a significant dynamic forcing on the atmospheric circulation from East Asia to the northeastern Pacific. When the storm track weakens in winter, the transient eddy-induced geopotential height tendency results in the southward movement and deepening of the East Asian trough and is conducive to the maintenance of the positive WP pattern at 500 hPa; it is also helpful for intensifying the Siberia High and Aleutian Low at 850 hPa. The transient eddy-induced zonal wind tendency tends to weaken the subtropical jet and strengthen the westerly flow in the north of the subtropical jet. All these factors are beneficial for strengthening the EAWM, which will cause low temperature in China.

## 5. Possible Causes of Intensity Anomaly of North Pacific Storm Track

SST can change the atmospheric baroclinicity through sensible heat and latent heat exchange, thus affecting the activities of the storm track. As shown in the regression of the SST field (Fig. 6), the SST decreases from the South China Sea to Kuroshio, and the areas passing the significance test are mainly located in the South China Sea and the starting area of Kuroshio. The correlation coefficient between the left-field time series of SVDI and the interannual component of the Kuroshio SST index is  $-0.36$ , which is significant at the 95% confidence level. This means that when the Kuroshio SST is lower (higher) than normal, the storm track weakens (strengthens). Zhu and Sun<sup>(49)</sup> also found that the SSTA over Kuroshio during winter exerts a crucial effect on the interannual variability in the vigor and meridional displacement of the central and western parts of the North Pacific storm track. Therefore, the Kuroshio SSTA may affect the intensity of the storm track, which is worthy of further study.

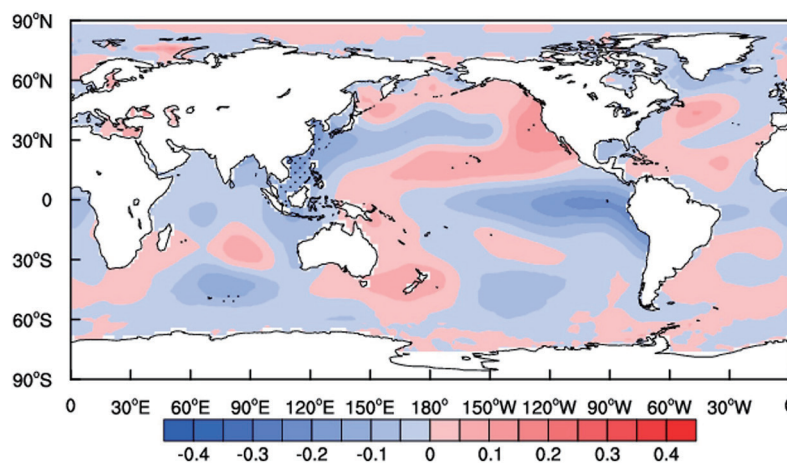


Fig. 6. (Color online) Regression of SST to the normalized time coefficient of the left field of SVDI. The dotted areas exceed the 95% confidence level.

## 6. Conclusions

On the basis of the daily average temperature data provided by the National Meteorological Information Center and NCEP/NCAR reanalysis data from 1961 to 2013, we analyzed the relationship between the North Pacific storm track and the winter temperature in China and its possible mechanism on the interannual scale by SVD, regression, and composite analyses. The main conclusions are as follows.

When the North Pacific storm track weakens (strengthens), the winter temperature in China is generally lower (higher). The intensity of the North Pacific storm track in winter is closely related to the atmospheric circulation from East Asia to the North Pacific. When the storm track weakens in winter, the main characteristics of the abnormal atmospheric circulation are the positive EU and WP patterns, meridional circulation in the middle-high latitude at 500 hPa, weakening polar front jet and strengthening subtropical jet at 300 hPa, and intensified Siberia High and Aleutian Low at sea-level pressure, which make the EAWM stronger. Moreover, a cold mass is formed in the south of Lake Baikal and results in low-temperature weather in China.

The dynamic forcing of transient eddy along the storm track is important for the formation and maintenance of the atmospheric circulation. The possible mechanism of the storm track intensity anomaly affecting the winter temperature in China is that when the storm track weakens, the dynamic forcing of the transient eddy is conducive to the maintenance of the positive phase of WP teleconnection, leading to the deepening and southward movement of the East Asian trough and the strengthening of the Siberia High and Aleutian Low. The forcing of the transient eddy on the westerly flow tends to strengthen the subtropical jet and weaken the westerly flow on the north side of the subtropical jet. The anomalous centers of atmospheric circulation induced by the transient eddy are basically the same as that of the actual atmospheric circulation, which are conducive to the strengthening of the winter monsoon, leading to a wide range of low-temperature weather in China. The Kuroshio SSTA may affect the intensity of the storm track, which is worthy of further study.

This research is based on the observation data from 1961 to 2013 provided by the National Natural Science Foundation of China. Owing to the recent development of observation instruments and sensors, the quality and resolution of observation data have improved considerably. It is suggested that further research be initiated to analyze the data collected in recent years.

## Acknowledgments

This research work was funded by the National Natural Science Foundation of China (41575070 & 41075070), Specialized Scientific Research for Public Welfare Industry (Meteorological Sector) (GYHY201306028), and Priority Academic Program Development (PAPD) of Jiangsu Higher Education Institutions.

## References

- 1 E. K. M. Chang and Y. F. Fu: *J. Clim.* **15** (2002) 642.
- 2 X. Ma and Y. Zhang: *Clim. Dyn.* **51** (2018) 3685.
- 3 Y. Yao, Z. Zhong, X. Q. Yang, and X. Huang: *Theor. Appl. Clim.* **136** (2019) 1249.
- 4 C. Li and J. J. Wettstein: *J. Clim.* **25** (2012) 1587.
- 5 Y. Xiang and X. Yang: *Adv. Atmos. Sci.* **29** (2012) 484.
- 6 J. Song, C. Li, and J. Pan: *J. Clim.* **24** (2011) 1239.
- 7 C. Liu, X. Ren, and X. Yang: *Adv Atmos Sci.* **31** (2014) 197.
- 8 Q. Chen, H. Hu, and X. Ren: *J. Geophys. Res. Atmos.* **124** (2019) 4891.
- 9 H. Nakamura, T. Izumi, and T. Sampe: *J. Clim.* **15** (2002) 1855.
- 10 S. X. Zhang and X. J. Ren: *J. Meteorol. Sci.* **37** (2017) 1.
- 11 N. C. Lau: *J. Atmos. Sci.* **45** (1988) 2718.
- 12 N. Shi: *J. Atmos. Sci.* **37** (2013) 1187.
- 13 H. Nakamura and A. Shimpo: *J. Clim.* **17** (2004) 1828.
- 14 T. Sampe, H. Nakamura, A. Goto, and W. Ohfuchi: *J. Clim.* **23** (2010) 1793.
- 15 J. Saulière, D. J. Brayshaw, B. Hoskins, and M. Blackburn: *J. Atmos. Sci.* **69** (2012) 840.
- 16 C. Zhang, H. Liu, J. Xie, C. Li, and P. Lin: *Adv. Atmos. Sci.* **37** (2020) 1256.
- 17 D. Y. He, X. L. Den, and W. J. Zhu: *Bull. Mar. Sci.* **11** (2009) 1.
- 18 M. Y. Liu, C. Y. Li, and X. Chen: *Hai Yang Xue Bao.* **75** (2017) 98.
- 19 T. Sampe, H. Nakamura, A. Goto, and W. Ohfuchi: *J. Clim.* **23** (2010) 1793.
- 20 L. Y. Wang, H. B. Hu, and X. Q. Yang: *Clim. Dyn.* **52** (2019) 5623.
- 21 J. Fang and X. Q. Yang: *Clim. Dyn.* **47** (2016) 1989.
- 22 W. H. Qian: *Chi. J. Geophys.* **55** (2012) 1439. <https://doi.org/10.6038/j.issn.0001-5733.2012.05.002>
- 23 H. S. Chen, L. Liu, and Y. J. Zhu: *Sci. China Earth Sci.* **42** (2012) 1951. <https://doi.org/10.1007/s11430-012-4442-z>
- 24 X. Y. Zhou, W. J. Zhu, and C. Gu: *Chin. J. Atmos. Sci.* **39** (2015) 978.
- 25 Z. J. Zhang and W. H. Qian: *Chin. J. Atmos. Sci.* **36** (2012) 1269.
- 26 C. Wang and Z. B. Sun: *Chin. J. Atmos. Sci.* **36** (2016) 301.
- 27 C. Wang, Z. B. Sun, and N. Wang: *Chin. J. Atmos. Sci.* **40** (2016) 401.
- 28 M. Jiang, X. Liu, H. Wang, and Y. Huang: *Sens. Mater.* **32** (2020) 4471. <https://doi.org/10.18494/SAM.2020.3126>
- 29 W. G. Jeon and E. M. Kim: *Sens. Mater.* **31** (2019) 3289. <https://doi.org/10.18494/SAM.2019.2433>
- 30 Y. Takei, Y. Hiroyuki, K. Hirasawa, H. Nanto, and K. Wada: *Sens. Mater.* **28** (2020) 237.
- 31 C. Huang, J. Li, X. Wang, J. Liao, H. Yu, C. C. Chen, and K. C. Wang: *Sens. Mater.* **33** (2021) 2365.
- 32 H. Gong, L. Wang, W. Zhou, W. Chen, R. Wu, and L. Liu: *J. Clim.* **31** (2018) 9001.
- 33 X. Shi, J. Sun, D. Wu, L. Yi, and D. Wei: *J. Ocean Univ. Chin.* **14** (2015) 604.
- 34 L. Zhang, Y. Liu, and F. Zhao: *Stoch Environ. Res Risk Assess.* **32** (2018) 733.
- 35 Z. B. Sun: *The Statistical Features of the 40-60 Days Fluctuations* (China Ocean Press, Beijing, 1992) 29.
- 36 Y. G. Ding and Z. H. Jiang: *Time Series Signal Processing of Meteorological Data* (China Meteorological Press, Beijing, 1998) p. 32.
- 37 Y. Li, W. J. Zhu, and J. S. Wei: *J. Meteorol. Sci.* **34** (2010) 1001.
- 38 J. M. Wallace and D. S. Gutzler: *Mon. Weather Rev.* **109** (1981) 784.
- 39 L. Wang and W. Chen: *J. Clim.* **27** (2014) 2361.
- 40 Z. X. Li and Z. B. Sun: *J. Nanjing Inst. Meteorol.* **27** (2004) 145.
- 41 N. C. Lau and E. O. Holopainen: *J. Atmos. Sci.* **41** (1984) 313.
- 42 G. J. Yang, X. J. Ren, and X. G. Sun: *J. Meteorol. Sci.* **30** (2010) 285.
- 43 Y. Li and N. C. Lau: *J. Clim.* **25** (2012) 4993.
- 44 L. Y. Wang, H. B. Hu, X. Q. Yang, and X. Ren: *J. Atmos. Sci.* **46** (2016) 1658.
- 45 G. R. North, T. L. Bell, R. F. Cahalan, and F. J. Moeng: *Mon. Weather Rev.* **110** (1982) 699.
- 46 Y. Y. Liu and W. Chen: *Chin. J. Atmos. Sci.* **36** (2012) 423.
- 47 Y. Li, H. E. Yong, J. H. He, and A. J. Jiang: *J. Meteorol. Sci.* **27** (2007) 119.
- 48 S. Tanaka, K. Nishii, and H. Nakamura: *J. Clim.* **29** (2016) 6597.
- 49 W. J. Zhu and Z. B. Sun: *Hai Yang Xue Bao.* **58** (2000) 309.